

The effect of cellular cholesterol on membrane-cytoskeleton adhesion

Mingzhai Sun¹, Nathan Northup¹, Françoise Marga¹, Tamas Huber², Fitzroy J. Byfield³, Irena Levitan⁴ and Gabor Forgacs^{1,5,*}

¹Department of Physics and Astronomy, University of Missouri-Columbia, Columbia, MO 65211, USA

²Department of Biophysics, University of Pecs, H-7624, Hungary

³Institute of Medicine and Engineering, Department of Pathology and Laboratory Medicine, University of Pennsylvania, Philadelphia, PA 19104, USA

⁴Pulmonary, Critical Care and Sleep Medicine, University of Illinois at Chicago, Chicago, IL 60612, USA

⁵Department of Biological Sciences, University of Missouri-Columbia, Columbia, MO 65211, USA

*Author for correspondence (e-mail: forgacs@missouri.edu)

Accepted 27 April 2007

Journal of Cell Science 120, 2223-2231 Published by The Company of Biologists 2007

doi:10.1242/jcs.001370

Summary

Whereas recent studies suggest that cholesterol plays important role in the regulation of membrane proteins, its effect on the interaction of the cell membrane with the underlying cytoskeleton is not well understood. Here, we investigated this by measuring the forces needed to extract nanotubes (tethers) from the plasma membrane, using atomic force microscopy. The magnitude of these forces provided a direct measure of cell stiffness, cell membrane effective surface viscosity and association with the underlying cytoskeleton. Furthermore, we measured the lateral diffusion constant of a lipid analog DiI_{C12}, using fluorescence recovery after photobleaching, which offers additional information on the organization of the membrane. We found that cholesterol depletion significantly increased the adhesion energy between the

membrane and the cytoskeleton and decreased the membrane diffusion constant. An increase in cellular cholesterol to a level higher than that in control cells led to a decrease in the adhesion energy and the membrane surface viscosity. Disassembly of the actin network abrogated all the observed effects, suggesting that cholesterol affects the mechanical properties of a cell through the underlying cytoskeleton. The results of these quantitative studies may help to better understand the biomechanical processes accompanying the development of atherosclerosis.

Key words: Cholesterol, Membrane tethers, Membrane-cytoskeleton adhesion, Atomic force microscopy (AFM), Fluorescence recovery after photobleaching (FRAP), Atherosclerosis

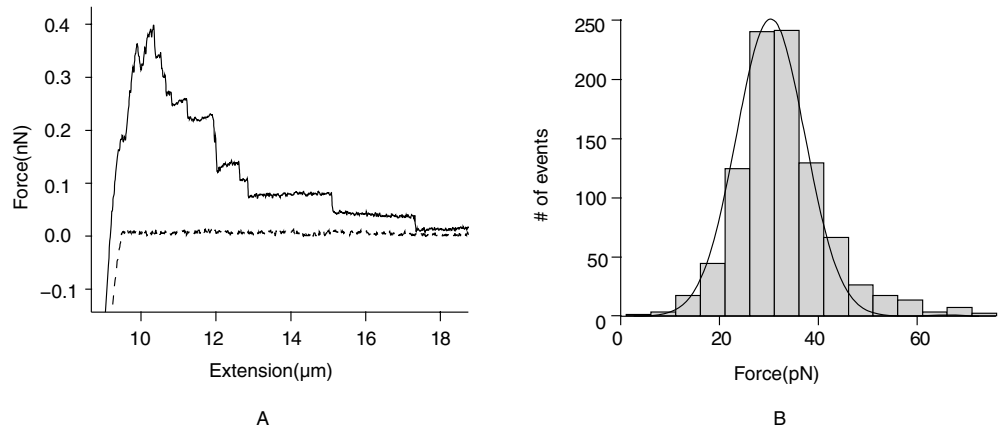
Introduction

Membrane cholesterol is an important factor in determining the physical properties of the lipid bilayer, such as its fluidity (Brulet and McConnell, 1976; Cooper, 1978; Xu and London, 2000) and elasticity (Evans and Needham, 1987; Needham and Nunn, 1990). Specifically, in the case of artificial vesicles, addition of cholesterol increases membrane stiffness (Needham and Nunn, 1990). However, in contrast to model membranes, Byfield et al. (Byfield et al., 2004) demonstrated that cholesterol depletion of bovine aortic endothelial cells significantly decreased cell deformability, as assessed by measuring the length of membrane deformation aspirated into a glass micropipette. Latrunculin-A-induced disassembly of the F-actin network abrogated the stiffening effect. Since these micropipette aspiration experiments affect the cell globally they do not allow determination of whether the stiffening effect of cholesterol depletion is due to the reorganization of the cytoskeleton, the modifications in membrane-cytoskeleton interaction or both. Several studies showed the effect of cholesterol on lateral protein diffusion (Goodwin et al., 2005; Shvartsman et al., 2006). In particular, Kwik and co-workers (Kwik et al., 2003) demonstrated that membrane cholesterol depletion decreased protein mobility in the membrane of skin fibroblasts and this effect resulted from changes in the architecture of the underlying actin network, again implicating

the cytoskeleton. These observations clearly illustrate that cholesterol manipulation affects cells more globally than just through their membranes (Kwik et al., 2003).

In the present study we used AFM-based force spectroscopy to quantitatively investigate the effect of cholesterol on membrane-cytoskeleton adhesion, a factor that controls vital cellular functions, such as endocytosis, exocytosis, lamellipodial retraction and extension, and cell migration (Sheetz, 2001). Specifically, membrane nanotubes (i.e. tethers) were extracted from endothelial cells whose mechanical properties are major determinants of vascular functions, such as flow-induced vasodilatation and vascular remodeling (Chien and Shyy, 1998; Davies et al., 1995; Sieminski et al., 2004). Membrane nanotubes have been studied extensively by a number of techniques, such as optical tweezers (Dai and Sheetz, 1995; Raucher and Sheetz, 2000; Inaba et al., 2005; Titushkin and Cho, 2006), magnetic tweezers (Heinrich and Waugh, 1996; Hosu et al., 2007), aspirating micropipettes (Shao and Hochmuth, 1996; Girdhar and Shao, 2004; Xu and Shao, 2005) and AFM (Puech et al., 2005; Sun et al., 2005), in a wide range of cell types including red blood cells (Hochmuth et al., 1982), neutrophils (Zhelev and Hochmuth, 1995; Shao and Xu, 2002), neurons (Hochmuth et al., 1996; Dai and Sheetz, 1995; Dai et al., 1998), fibroblasts (Raucher and Sheetz, 1999; Raucher and Sheetz, 2001), endothelial cells

Fig. 1. (A) A typical force vs extension curve. The dotted line corresponds to the approach curve and the solid line is the retraction curve. On the retraction curve, several step-like structures are clearly discernible, which correspond to the sequential detachment of individual tethers from the cantilever. (In principle these steps could signal the detachment of a single tether with multiple connections to the cantilever. This possibility can be excluded on the basis of the numerous earlier studies in which single tethers were extracted and no steps in the course of tether elongation were observed.) The shown retraction curve corresponds to an experiment performed with a control cell at 3 $\mu\text{m}/\text{second}$. (B) Histogram constructed from the data (size of the steps) collected in the control experiments at 3 $\mu\text{m}/\text{second}$. The solid line is the Gaussian fit to the histogram, which gives the mean value of the tether force, 33 pN.



(Girdhar and Shao, 2004), tumor cells (Sun et al., 2005; Hosu et al., 2007) and stem cells (Titushkin and Cho, 2006). Membrane tethers are of interest because of their many biological functions, such as providing intercellular and intracellular communication channels (Polishchuk et al., 2003; Rustom et al., 2004; Upadhyaya and Sheetz, 2004; Vidulescu et al., 2004; White et al., 1999) and controlling the rolling along and attachment to the endothelial wall of leukocytes (Alon et al., 1998; Edmondson et al., 2005; Ramachandran et al., 2004). In the latter case they are formed through specific receptor-ligand bonds upon contact with endothelial cells or platelets (Schmidtke and Diamond, 2000).

In the AFM technique the force F (i.e. tether force) needed to pull a tether from the membrane at a constant velocity V_t is measured and then the dependence of F on V_t is analyzed (Brochard-Wyart et al., 2006; Evans et al., 2005; Heinrich et al., 2005; Hochmuth et al., 1996). In most cases this dependence is accurately described by the relationship $F = F_0 + 2\pi\eta_{\text{eff}}V_t$, which is used to evaluate the membrane surface viscosity η_{eff} and the threshold pulling force F_0 . Effective surface viscosity here means, that in general η_{eff} contains contributions associated with the intrinsic material properties of the lipid bilayer, the interbilayer slip and the association of the membrane with the underlying cytoskeleton (Hochmuth et al., 1996). The force F_0 is a direct measure of the membrane-cytoskeleton adhesion energy and membrane stiffness (Hochmuth et al., 1996; Sheetz, 2001). Thus both F_0 and η_{eff} contain information on the interaction of the membrane with the cytoskeleton. AFM can exert considerably larger forces ($\sim\text{nN}$) than optical tweezers (<500 pN) and it is more accurate than aspirating micropipettes. Using this method, we quantified the membrane-cytoskeleton interaction in bovine aortic endothelial cells and determined the effective surface viscosities of cells with different levels of cholesterol content. In bulk liquids, viscosity and diffusion constant are inversely proportional to each other. To investigate this relationship in two-dimensional membranes, and gain additional information on the effects of cholesterol, fluorescence recovery after photobleaching (FRAP) (Axelrod et al., 1976; Edidin et al., 1976; Reits and Neefjes, 2001) was used to measure the lateral diffusion of a lipid analog DiI₁₂.

Results

Cholesterol depletion/enrichment significantly increases/decreases the threshold tether force

To investigate the effect of cholesterol on the biophysical properties of the endothelial plasma membrane, tether-pulling experiments were performed on control, cholesterol enriched and cholesterol-depleted cells. The mean tether force at each specific pulling speed was determined from the Gaussian fit to the resultant histogram (see Materials and Methods; Fig. 1B). Cell cholesterol level after cholesterol modulation was verified (Fig. 2A inset) as previously described (Levitan et al., 2000). The threshold tether force F_0 and the effective surface viscosity of the membrane, η_{eff} , were determined from the linear fit (Fig. 2A,C) to the data; their values are listed in Table 1 (the values for η_{eff} are comparable with those reported for other eukaryotic cells) (Li et al., 2002; Girdhar and Shao, 2004; Xu and Shao, 2005). Cholesterol treatment affected η_{eff} similarly at room temperature and 37°C: enrichment and depletion resulted in a decrease ($P < 0.05$) and no change ($P > 0.05$), respectively, in this quantity. As far as F_0 is concerned, at room temperature, cholesterol enrichment and depletion resulted in its decrease and increase, respectively. At 37°C, cholesterol depletion still resulted in the increase of F_0 ($P < 0.05$), whereas cholesterol enrichment did not seem to affect it ($P > 0.05$). Overall, the changes brought about by cholesterol treatment were less pronounced at 37°C than at room temperature. These findings demonstrate that cholesterol is an efficient regulator of the biophysical properties of the membrane. Furthermore, they imply that at physiological temperatures, cells are able to more effectively recover from cholesterol-caused perturbations.

Disruption of F-actin abrogates the effect of cholesterol on the tether force

Earlier studies have demonstrated that the tether force strongly depends on the integrity of the F-actin network (Dai et al., 1999; Dai and Sheetz, 1995; Sun et al., 2005). To test the F-actin dependence of the tether force, prior to pulling experiments, cells were exposed to 1 μM latrunculin A, an F-actin depolymerizing agent (Spector et al., 1989). As

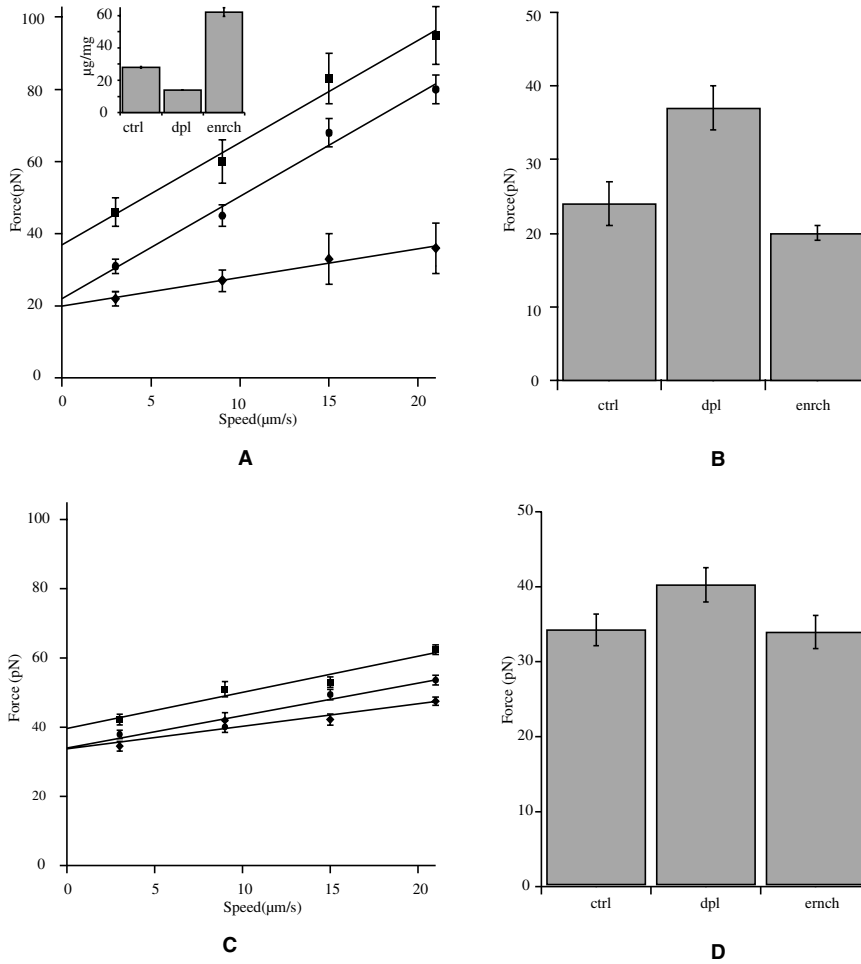


Fig. 2. (A,C) Tether force vs tether growth velocity at room temperature (A) and 37°C (C). The solid lines are linear fits to the corresponding data sets (control, ●; depletion, ■; enrichment, ◆). Inset in A, cholesterol level measured by GLC (see Materials and Methods). ctrl, control; dpl, cholesterol depleted; enrch, cholesterol enriched. The values of slopes ($\sim\eta_{eff}$) and intercepts (F_0) are listed in Table 1. (B,D) Bar graph for F_0 at room temperature (B) and 37°C (D). Error bars in A and C represent s.e. obtained from the experimental data points. Errors in the bar graphs represent the error of the linear fit to the data. All six R^2 values were larger than 0.97.

expected, fewer actin fibers were observed in latrunculin-A-treated cells (Fig. 3B, panels d-f). Although there was no latrunculin A in the CO₂-independent medium (in which the experiments were carried out), we did not observe cell recovery in either morphology or tether force, indicating that the drug remained in the cells for the entire duration of the measurements (1-1.5 hours; results not shown). Disruption of F-actin resulted in a significant reduction in F_0 and η_{eff} for both the control and cholesterol-depleted cells (Fig. 3A and Table 1). However, latrunculin A did not significantly affect these quantities in cholesterol-enriched cells. In addition, after latrunculin A treatment we found no statistical difference in F_0 and η_{eff} between control, cholesterol-depleted and cholesterol-enriched cells ($P>0.05$; Fig. 3A and Table 1). These results imply that the organization of the actin cytoskeleton strongly influences the biophysical properties of

the membrane in control and cholesterol-depleted cells, but has no significant effect in cholesterol-enriched cells.

Cellular cholesterol content affects cell morphology

DIC microscopy was used to study the effect of differential cholesterol treatment on cell morphology. Blind experiments (see Materials and Methods) were performed to minimize bias in the interpretation of the images. Cholesterol-depleted cells appeared smaller and thicker (Fig. 4A) than control cells (which were well spread, Fig. 4B), whereas cholesterol-enriched cells could be resolved by their increased blebbing (Fig. 4C). These findings suggest a correlation between cell membrane cholesterol content and membrane-cytoskeleton association or cytoskeleton organization. In particular, blebs in cholesterol-enriched cells may indicate weakened membrane-cytoskeleton association.

Table 1. Threshold pulling force (F_0) and effective surface viscosity (η_{eff})*

	F_0 (pN)			η_{eff} (pN second/ μ m)		
	37°C	22°C	+Lat A (22°C)	37°C	22°C	+Lat A (22°C)
Control	34±2	24±4	14±2	0.15±0.03	0.5±0.05	0.1±0.04
Cholesterol depleted	40±2	37±3	17±1	0.16±0.03	0.4±0.05	0.1±0.02
Cholesterol enriched	34±1	20±1	18±1	0.10±0.02	0.1±0.02	0.1±0.02

*Data are means ± s.d. Lat A, latrunculin A.

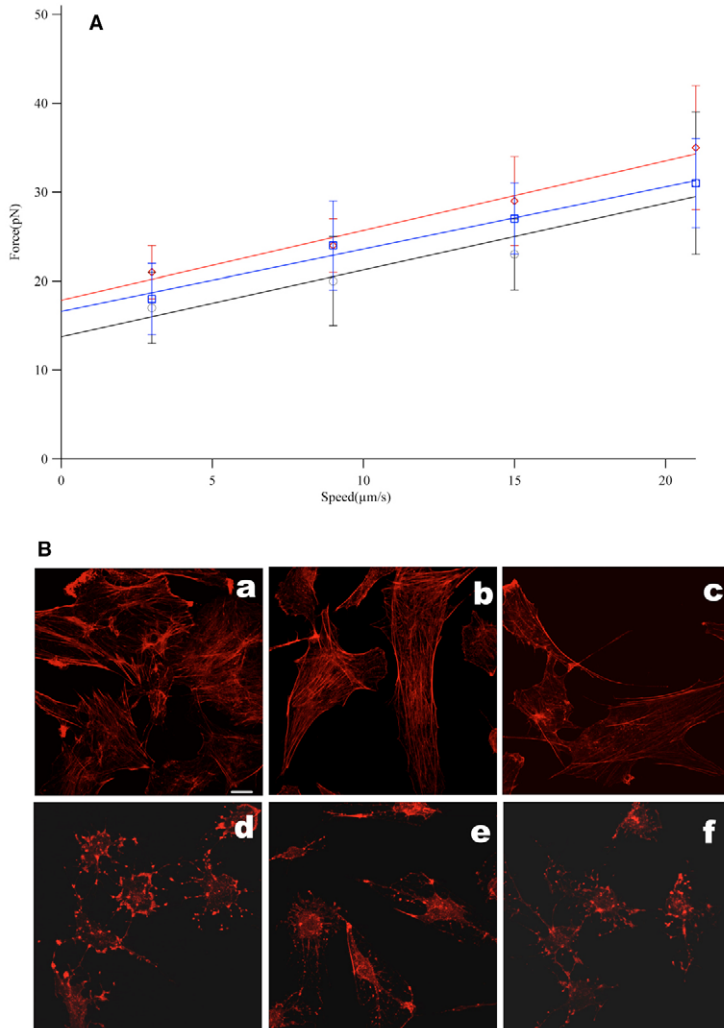


Fig. 3. (A) Tether force vs tether growth velocity after latrunculin A treatment (○, control; □, cholesterol depleted; △, cholesterol enriched). Values of the intercepts and slopes are listed in Table 1. Error bars represent s.e. (note that the error bars overlap). (B) Confocal images of the actin cytoskeleton for control (a,d), cholesterol-depleted (b,e), cholesterol-enriched (c,f) BAECs, without (top row) or with (bottom row) latrunculin A treatment. Bar, 10 µm.

Cellular cholesterol content affects variability in tethers

If the plasma membrane were not connected to the cytoskeleton (the case of artificial lipid vesicles), no differences between tethers would be expected. Thus, variability in tethers could also provide information on membrane-cytoskeleton association. Therefore, we performed a systematic study on the width of the histograms, constructed from the step-like events shown in Fig. 1, in all treatment cases. (As the analysis presented in the Materials and Methods showed, the width is mainly determined by the variability in tethers.) As results in Table 2 show, cholesterol depletion significantly increased variability, whereas cholesterol enrichment had a much smaller effect. Latrunculin A treatment renders cells considerably more homogeneous in all three cases (control, depletion and enrichment). These findings are

consistent with the results presented earlier. Cholesterol depletion enhances membrane-cytoskeleton interaction and thus makes tethers less homogeneous. Upon latrunculin A treatment, this enhanced membrane-cytoskeleton interaction is abrogated and, as a consequence, tethers become more homogeneous.

Cholesterol depletion suppresses lateral diffusion in the membrane

Diffusion (e.g. of proteins) in the membrane is important in a number of cellular processes, such as signaling and adhesion. To investigate how cholesterol depletion or enrichment affects this transport mechanism, cells were labelled with DiIC₁₂ for FRAP measurements, as described in the Materials and Methods. Analysis of the recovery curves after photobleaching (Siggia et al., 2000) (Fig. 5A) revealed that cholesterol depletion resulted in the decrease of DiIC₁₂ lateral mobility ($P < 0.05$; Fig. 5B), whereas cholesterol enrichment had no statistically significant effect (Fig. 5B). Disruption of F-actin with latrunculin A had little to no effect on DiIC₁₂ mobility for either control or cholesterol-enriched cells (Fig. 5B). However, latrunculin A treatment of cholesterol-depleted cells resulted in a significant increase in the diffusion coefficient (Fig. 5B). Furthermore, similarly to the threshold tether force and effective surface viscosity, after latrunculin A treatment we found no statistical difference in the values of the diffusion constants among control, cholesterol-depleted and cholesterol-enriched cells. Interestingly, our findings contrast with those of Goodwin and co-workers (Goodwin et al., 2005). These investigators observed decreased diffusion of DiIC₁₆ and DiIC₁₈ in the membrane of fibroblasts upon cholesterol enrichment and no change upon cholesterol depletion. This may imply different membrane localization of these dyes or cell-specific response to cholesterol treatment. However, our results are consistent with enhanced membrane-cytoskeleton adhesion upon cholesterol depletion (see Discussion).

Cholesterol enrichment reduces bond force

Earlier work has confirmed that tether formation can reduce the force exerted on the specific bonds (the bond force, F_b) between endothelial cells of the vascular wall and leukocytes, and thus result in increased chance of adherence between the two cell types (Girdhar and Shao, 2004; Ramachandran et al., 2004; Schmidtke and Diamond, 2000; Shao et al., 1998). To clarify how this finding may be affected by differential cholesterol conditions, we determined the time dependence of L (tether length) and F_b for tethers connecting a leukocyte to an endothelial cell (see Materials and Methods). We found that after cholesterol enrichment, L and F_b respectively increase (Fig. 6A) and decrease (Fig. 6B) much faster than in the case of control and cholesterol-depleted cells. This result is consistent with the finding that cholesterol enrichment leads to decreased effective surface viscosity (Fig. 2A,C). Interestingly, cholesterol depletion had no strong effect on either L or F_b . Increased tether length and reduced bond force both favor the slowing down of circulating leukocytes

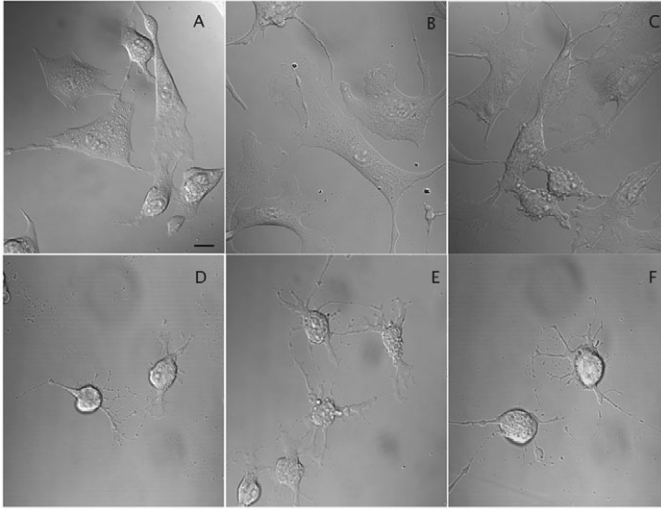


Fig. 4. DIC images of cells with different cholesterol content. Cholesterol-depleted (A,D), control (B,E), cholesterol-enriched (C,F) BAECs, without (top row) or with (bottom row) latrunculin A treatment. Latrunculin-A-treated cells show a similar spherical morphology independently of cholesterol content. Bar, 10 μm .

and, as a consequence, the possible accumulation of cells in the vicinity of the endothelium. Thus, increase in the endothelial cell membrane cholesterol level may be an initial step in atherosclerotic plaque formation.

Discussion

Formation of membrane tethers requires significant changes in membrane curvature. The associated energy cost depends on the biomechanical properties of the bilayer, as well as its association with the cytoskeleton (Dai and Sheetz, 1995; Hochmuth et al., 1996; Sheetz, 2001). By pulling membrane tethers from bovine aortic endothelial cells using AFM, we have shown that cholesterol depletion significantly increases membrane stiffness (and thus makes the pulling of tethers harder), whereas cholesterol enrichment weakens it. These

Table 2. Tether variability*

	S_{total}
Control	7.1
Control + Lat A	6.4
Cholesterol depleted	22.9
Cholesterol depleted + Lat A	10.2
Cholesterol enriched	8.7
Cholesterol enriched + Lat A	7.5

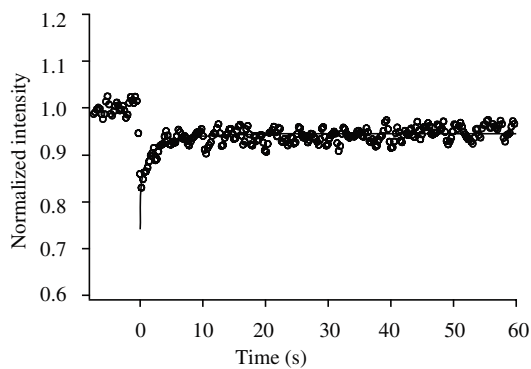
*Results are given in terms of the width (standard deviation, S_{total}) of the Gaussian fit to the histograms, as explained in the Materials and Methods. Lat A, latrunculin A.

findings are consistent with those of Byfield et al. (Byfield et al., 2004), who used micropipette aspiration to quantify the effect of cholesterol. Using the same technique, Needham and Nunn (Needham and Nunn, 1990), however, found that elevation of membrane cholesterol increases the stiffness of artificial lipid bilayers. We have also shown that, unexpectedly, cholesterol enrichment decreases the effective surface viscosity of the membrane, whereas cholesterol depletion has practically no effect on this quantity. Finally, we have demonstrated that cholesterol depletion (but not cholesterol enrichment) affects lateral membrane diffusion. Taken together, these findings imply that changes in the level of membrane cholesterol have profound effects on membrane-cytoskeleton interaction. Thus, cholesterol affects the cell not only locally, but also globally through the cytoskeleton.

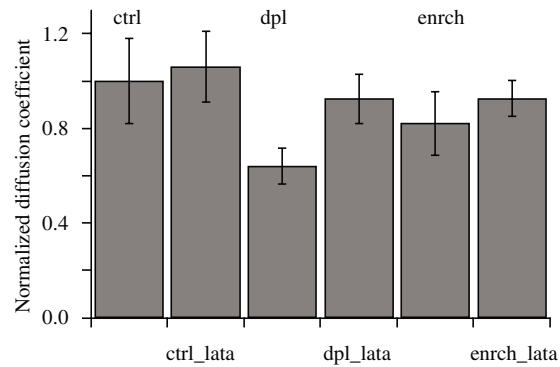
The contribution to the tether force by membrane-cytoskeleton adhesion, F_{ad} , can be estimated as follows:

$$F_{ad} = F_0 - F_0^{lata}, \quad (1)$$

where F_0 and F_0^{lata} are the threshold tether force before and after latrunculin A treatment, respectively. Since latrunculin A treatment leads to the disruption of the F-actin network (Fig. 3B, panel d-f), F_{ad} is a quantitative measure for the strength of the membrane-cytoskeleton interaction. The values of F_{ad} for control, depleted and enriched cells were 10, 20 and 2 pN, respectively (Fig. 7). The high value of F_{ad} for cholesterol depletion and the lower value for cholesterol enrichment



A



B

Fig. 5. (A) A typical recovery curve in a control FRAP experiment. The fluorescence intensity is normalized to the average fluorescence intensity before photobleaching. (B) Diffusion coefficients in the various treatment cases (normalized to the value for the control). ctrl, control; dpl, cholesterol depleted; enrch, cholesterol enriched; lata, latrunculin A treated.

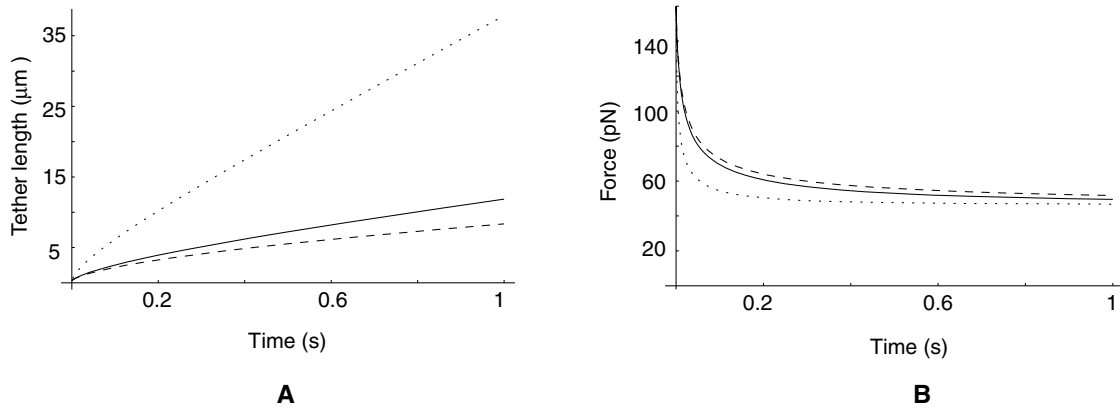


Fig. 6. (A) Tether length vs time, calculated using equation 2 (see Materials and Methods). The tether grows much faster after cholesterol enrichment (dotted line) compared with the control (solid line) and cholesterol-depleted (dashed line) cases. The curves for control and cholesterol depletion are similar. (B) The estimated force acting on a bond between an endothelial tether and a leukocyte. After cholesterol enrichment (dotted curve), initially, the bond force decreases much faster than in the control (solid curve) and cholesterol depleted (dashed curve) cases. The curves for the control and cholesterol depletion are again similar.

indicate strong and weak interaction, respectively, between the membrane and cytoskeleton. Membrane-cytoskeleton interaction is essential for the membrane to conform to the cytoskeleton; its weakening leads to blebbing (Sheetz et al., 2006). Our studies using DIC imaging (Fig. 4C), indeed show this to happen in cholesterol-enriched cells.

Another important finding of this study is that cholesterol enrichment results in a significant decrease in effective surface viscosity, η_{eff} , whereas cholesterol depletion has no effect. The effective membrane surface viscosity is determined by multiple factors, such as intrinsic membrane properties, inter-bilayer slip, and the slip between the membrane and cytoskeleton (Hochmuth et al., 1996). Among these three contributions, the most significant is the slip between the membrane and cytoskeleton, as shown by Marcus (Marcus and Hochmuth, 2002), where latrunculin A treatment of neutrophils was found to decrease η_{eff} from 1.1 pN \times second/ μ m to close to zero. Our

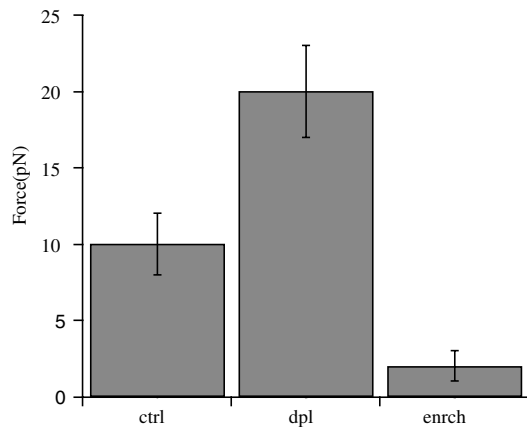


Fig. 7. The estimated membrane-cytoskeleton adhesion force, F_{ad} , calculated using equation 1. Values of F_{ad} for cholesterol-depleted (dpl) and cholesterol-enriched (enrch) cells are both significantly ($P < 0.05$) different from the control (ctrl).

experiments support this finding: after 1 μ M latrunculin A treatment, η_{eff} decreases from 0.5 to about 0.1 pN \times second/ μ m for the control and cholesterol-depleted cells. The decrease in η_{eff} is most probably due to the loss of bonds linking the membrane to the cytoskeleton (Marcus and Hochmuth, 2002; Raucher et al., 2000). Therefore, the decrease in η_{eff} in cholesterol-enriched cells is consistent with the assumption that under such conditions membrane-cytoskeleton adhesion is reduced. The fact that no further decrease in the effective membrane viscosity is observed upon latrunculin A treatment in cholesterol-enriched cells (Table 1), suggests that enrichment itself has already significantly decreased the membrane-cytoskeleton adhesion, making additional latrunculin A treatment largely ineffective. Interestingly, we found that the increase in F_{ad} in cholesterol-depleted cells is not accompanied with increase in η_{eff} . One possible explanation for this observation is that the increase in the component of η_{eff} owing to the slip between the cytoskeleton and the inner leaflet of the membrane (as consequence of increased membrane-cytoskeleton adhesion) is compensated by an opposite effect on one of the other components (see above).

The tether-pulling experiments were performed at both room temperature and physiological temperature. Although the main conclusions on the effect of cholesterol on cellular biophysical properties obtained in these experiments are valid in both cases, it is instructive to note that the differences between the various treatment cases are less pronounced at 37°C. This observation suggests that cells are capable to adapt to perturbations more effectively at physiological temperatures and the interpretation of experimental results obtained at room temperature has to be done with appropriate care.

Another approach to address the role of membrane cholesterol in determining membrane fluidity is measuring the lateral diffusion of lipid molecules using FRAP. Our study shows that after cholesterol depletion, the lateral diffusion of DiIC₁₂ decreased by about 30%, whereas cholesterol enrichment had no significant effect (Fig. 5B). These observations are consistent with earlier studies showing that

cholesterol depletion increases the immobile fraction of HLA I proteins (Kwik et al., 2003) and decreases the diffusion coefficient of both raft and non-raft proteins (Kenworthy et al., 2004; Vrljic et al., 2005). Cholesterol enrichment was shown to have no effect on the lateral diffusion coefficients of either membrane proteins or membrane lipids (Kenworthy et al., 2004; Vrljic et al., 2005). Also, consistently with the earlier studies, disassembly of the actin network abrogated the differences in the diffusion coefficients between cholesterol-depleted, cholesterol-enriched and control cells (Fig. 5B). This implies, in particular, that the suppression of lateral diffusion of DiIC₁₂ after cholesterol depletion is also related to the cytoskeleton.

An intriguing question is why the impact of cholesterol on η_{eff} , as measured by AFM, is different from its impact on D , as measured by FRAP. On theoretical grounds, it is expected that an increase in D implies a decrease in η_{eff} (Saffman and Delbruck, 1975). However, in our study, cholesterol enrichment significantly reduced η_{eff} , but had no appreciable effect on D . Conversely, cholesterol depletion had no effect on η_{eff} , but significantly decreased D . One possible explanation is that AFM and FRAP measure distinct membrane properties. A more profound reason may be that our FRAP study tests only the outer leaflet of the plasma membrane (where the diffusion of DiIC₁₂ takes place), whereas AFM tests both (since tethers and thus η_{eff} are sensitive to the interconnection between the two leaflets). Therefore, the outcome of the FRAP experiments is affected less by membrane-cytoskeleton adhesion. Indeed, results in Fig. 5B show a slight increase in D for control and enriched cells upon latrunculin A treatment. In cholesterol-depleted cells enhanced membrane-cytoskeleton adhesion may affect the movement of a lipid molecule even in the outer leaflet. Upon dismantling this adhesion, D becomes the same as in the other two cases. (The reason why depletion does not affect η_{eff} was discussed earlier.)

Changes in membrane-cytoskeleton adhesion are expected to have major impact on numerous cell functions (Sheetz, 2001). In particular, it is likely that an increase in membrane-cytoskeleton adhesion (e.g. by cholesterol depletion) makes it more difficult to form endocytic vesicles, slows down the rate of endocytosis, prevents the formation of membrane processes (such as lamellipodia protrusion) and affects cell morphology. Consistent with this expectation is the finding that cholesterol depletion reduces the rate of internalization of transferrin receptors by preventing coated pits to detach from the plasma membrane (Subtil et al., 1999). Conversely, cholesterol enrichment enhances endocytosis (Sharma et al., 2004). It is also important to note that although depleting cellular cholesterol with M β CD is not physiological, it was shown that exposing endothelial cells to oxLDL results in cholesterol depletion from endothelial caveolae (Blair et al., 1999). Furthermore, the effects of M β CD-induced cholesterol depletion on endothelial biomechanics are remarkably similar to those induced by oxLDL (Byfield et al., 2006).

Reduced membrane-cytoskeleton adhesion and decreased effective surface viscosity may have important implications in the development of atherosclerosis. Adhesion of circulating monocytes to the endothelium and consequent reduction in their rolling are important components in the atherogenic process (Cybulsky and Gimbrone, 1991;

Gimbrone et al., 1995; Rosenfeld et al., 1987). Experiments and numerical simulations demonstrate that formation of membrane tethers reduces the force exerted on specific bonds (i.e. selectin-PSGL1) and increases bond lifetime, which results in increased chance of adherence of neutrophils to the endothelium (Girdhar and Shao, 2004; Ramachandran et al., 2004; Schmidtke and Diamond, 2000; Shao, 1998). Our model calculation illustrates that after cholesterol enrichment, the force exerted on the specific bond formed between an endothelial tether and a leukocyte decreases much faster than in the control or depleted cases (Fig. 6B). As a consequence, bond lifetime increases, facilitating and stabilizing the rolling process. This suggests that cholesterol enrichment may increase the probability of adherence of monocytes to endothelium, an observation consistent with experimental findings (Pritchard et al., 1991a; Pritchard et al., 1991b).

In conclusion, based on AFM tether-pulling and FRAP measurements, we showed that alterations in the level of membrane cholesterol lead to significant changes in membrane-cytoskeleton adhesion, which in turn may affect important cellular and physiological processes. The molecular mechanisms, that control and regulate these effects, however, need further investigation.

Materials and Methods

Cell culture

Bovine aortic endothelial cells (BAECs; Cambrex East Rutherford, NJ) between passages 12 and 16 were grown in DMEM (Invitrogen, Carlsbad, CA) containing 10% fetal bovine serum (FBS; Sigma-Aldrich, St Louis, MO), 10 μ g/ml penicillin, streptomycin and kanamycin sulfate (Invitrogen, Carlsbad, CA). Cell cultures were maintained in a humidified incubator at 37°C, with 5% CO₂. Cells were split every 3–4 days.

Modulation of cellular cholesterol level

BAECs were enriched with or depleted of cholesterol by incubation with methyl- β -cyclodextrin (M β CD) saturated in cholesterol or using M β CD not complexed with cholesterol, as described in previous studies (Leviton et al., 2000). Free cholesterol mass analysis was done by gas-liquid chromatography (GLC) (Leviton et al., 2000). Cell protein content was determined on the lipid-extracted monolayer using a modification of the method of Lowry et al. (Lowry et al., 1951). All mass values were normalized on the basis of cell protein.

Tether force measurement

Measurements were performed as described earlier (Sun et al., 2005) both at room temperature and 37°C (assured by use of an enclosure with a thermostat surrounding the AFM workstation). Briefly, the in-house-built AFM was mounted on the stage of an Olympus IX70 inverted microscope. Each silicon nitride cantilever (Veeco, Santa Barbara, CA) used in the experiments was calibrated before a given measurement using thermal noise amplitude analysis (Butt and Jaschke, 1995; Hutter and Bechhoefer, 1993). The measured spring constants were between 8 and 12 mN/m, in good agreement with the nominal value of 10 mN/m, provided by the manufacturer. A 60-mm Petri dish containing cells in CO₂-independent medium at room temperature, supplemented with 10 μ g/ml penicillin, streptomycin, and kanamycin sulphate, was placed under the AFM. The cantilever was lowered toward the cell until contact was established. Contact was maintained for 2 to 30 seconds, after which the cantilever was retracted at a constant speed (3, 9, 15 and 21 μ m/second were used in the experiments). A typical retraction resulted in a series of step-like discontinuities (Fig. 1A). The step size corresponds to the force needed to pull a single tether, in particular the last one. Several hundred step-like events were recorded using 15–50 cells, with each cell subjected to multiple retraction experiments. Data analysis was carried out with Igor 4.09 (WaveMetrics, Lake Oswego, OR).

Determination of membrane surface viscosity

With the AFM apparatus one directly measures the tether force F as function of the tether growth velocity V_t (in our case the AFM cantilever retraction speed), thus the function $F(V_t)$. The mean value of F was determined from the Gaussian fit to the histogram constructed from the recorded step-like events; at least 500 were used in the experiments at room temperature and (owing to the higher thermal noise) 1000 at 37°C. The width of the Gaussians was also analyzed, because this quantity

contains information on the spread of the data owing to variability in tethers, cells and experiments.

There are different theories for the analysis of the function $F(V_i)$, including power law (Brochard-Wyart et al., 2006; Evans et al., 2005; Heinrich et al., 2005) and linear relationship (Hochmuth et al., 1996). In our experimental regime, the linear relationship $F = F_0 + 2\pi\eta_{\text{eff}}V_i$ worked well. The effective viscosity η_{eff} and threshold-pulling force F_0 were then determined respectively from the slope and intercept of the line used to fit the data. The threshold force for extracting a tether is given by $F_0 = 2\pi\sqrt{2TB}$, where the apparent membrane tension T (similarly to η_{eff}) provides a measure of the membrane-cytoskeleton adhesion and B is the membrane-bending stiffness (Sheetz, 2001). (Note that the quantity T is analogous to surface tension. Thus it represents the energy needed to increase the membrane surface area by one unit.)

Cytoskeleton disruption

For cytoskeleton disruption experiments, cells were cultured at 37°C, 5% CO₂ in 1 μM latrunculin A solution in DMEM, containing 10 μg/ml penicillin, streptomycin, and kanamycin sulphate (Invitrogen). Cells were treated for 30 minutes prior to AFM measurements, which were performed in latrunculin-A-free CO₂-independent medium, at room temperature, as described above.

Confocal fluorescence recovery after photobleaching

For DiIC₁₂ labeling, cells were incubated with 0.5 μg/ml of DiIC₁₂ (stock 5 mg/ml in DMSO) in DMEM without FBS for 20 minutes. Confocal FRAP was performed as described by Kenworthy et al. (Kenworthy et al., 2004). Briefly, a Zeiss LSM 510 Meta NLO 2-photon confocal (Carl Zeiss, Thornwood, NY) was used with a 63× 1.4 NA Zeiss Plan Apochromat oil-immersion objective, at digital zoom of 2, scan speed of 10, with the pin-hole set at 1 Airy unit. Prebleach and postbleach images were acquired using low laser intensity (at 488 nm). Photobleaching was performed using 10 scans with the 800 nm Chameleon 2-photon laser system in a rectangular region of interest, 4 μm wide. All FRAP measurements were carried out in CO₂-independent medium at room temperature. In the case of cytoskeleton disruption experiments, prior to measurement, cells were treated for 10 minutes with latrunculin A, as described above. The effective diffusion coefficients were determined from the postbleach image series using a program that compares the experimental and simulated recoveries into the bleached region (Siggia et al., 2000).

Visualization of the actin cytoskeleton and cell morphology

To visualize the microfilament network, F-actin staining was performed using standard procedure. Cells were fixed in 4% paraformaldehyde (PFA) for 10 minutes, permeabilized with 0.1% Triton X-100 for 5 minutes, incubated with PBS (2% FBS) for 15 minutes, and subsequently with 0.1 μM Rhodamine-phalloidin (Sigma, St Louis, MO) for 20 minutes. After each step, samples were rinsed three times in PBS. Images were acquired using a Bio-Rad Radiance 2000 (Carl Zeiss Microimaging, Thornwood, NY) confocal system. Cell morphology as function of cholesterol treatment was visualized with Differential Interference Contrast (DIC) microscopy. Images were acquired using the DIC imaging module on the Zeiss LSM 510 Meta NLO 2-photon confocal (Carl Zeiss, Thornwood, NY) with a 63× 1.4 NA Zeiss Plan Apochromat oil-immersion objective. To minimize the bias, blind experiments were performed. Control and cholesterol-treated cells were cultured on the same cover glass (appropriately partitioned in two regions) by one individual and subsequently imaged by another without the knowledge of which region contained the treated or control cells.

Bond force computation

Leukocytes circulating in the blood flow occasionally collide with the endothelial wall, which may result in tether formation, from either the endothelial or leukocyte membrane. The force, as a result of shear stresses in the blood flow, acting on the adhesive bond between the tip of the tether and the apposing membrane (i.e. selectin-PSGL1 ligand), F_b , can considerably be reduced by the extension of the tether (Shao et al., 1998). We investigated how cholesterol, through its effect on the mechanical properties of endothelial tethers may influence F_b . Using the model of Shao et al. (Shao et al., 1998; Girdhar and Shao, 2004; Girdhar et al., 2007) and the quantities F_0 and η_{eff} from the tether-pulling experiments, F_b can be calculated from the following equation:

$$F_b(L) = F_0 + 2\pi\eta_{\text{eff}}\frac{dL}{dt}, \quad (2)$$

where $L(t)$ is the instantaneous tether length. The above equation follows from the conditions of force and torque balance for a rolling leukocyte (along with an equation expressing the geometry of the leukocyte's attachment to the endothelium, assuming attachment through a single tether). We solved equation 2 numerically for endothelial tethers, formed under various cholesterol conditions. In the computation, the radius of the leukocyte and shear stress as a result of blood flow were assumed to be 4.25 μm and 0.08 pN/μm² respectively.

Statistical analysis

Analysis of covariance was used to compare the results of tether-pulling experiments under different conditions. For the FRAP data comparison, a Student's t -test was used (Zar, 1999).

For the width of the histograms the following analysis was performed. Three independent experiments were carried out at $V_i = 3$ μm/second on three different days, with five different cells each day. In total, 15 cells and 943 tethers were recorded. Using all the data, a histogram was constructed and its variance, S^2_{total} (where S is s.d.) evaluated from the Gaussian fit. We then determined the contributions to S^2_{total} of the variances attributable to the different experiments (S^2_{ex}), cells (S^2_{cell}) and the tethers (S^2_{tether}), using the linear mixed effects model (Neter et al., 1996): $S^2_{\text{total}} = S^2_{\text{tether}} + S^2_{\text{cell}} + S^2_{\text{ex}}$. This analysis revealed that the width of the histogram is mainly determined by the variability in the tethers, $S^2_{\text{tether}} \approx 0.93S^2_{\text{total}}$. The error due to heterogeneity in the cells was considerably smaller ($S^2_{\text{cell}} \approx 0.07S^2_{\text{total}}$), whereas that due to differences in the experiments was almost negligible ($S^2_{\text{ex}} \approx 0.001S^2_{\text{total}}$).

The authors benefited from discussion with Michael Sheetz. This work was supported by the American Heart Association (M.S.), NIH-HL073965 (I.L.) and NSF EF-0526854 (G.F.).

References

- Alon, R., Chen, S., Fuhlbrigge, R., Puri, K. D. and Springer, T. A. (1998). The kinetics and shear threshold of transient and rolling interactions of L-selectin with its ligand on leukocytes. *Proc. Natl. Acad. Sci. USA* **95**, 11631-11636.
- Axelrod, D., Ravidin, P., Koppel, D. E., Schlessinger, J., Webb, W. W., Elson, E. L. and Podleski, T. R. (1976). Lateral motion of fluorescently labeled acetylcholine receptors in membranes of developing muscle fibers. *Proc. Natl. Acad. Sci. USA* **73**, 4594-4598.
- Blair, A., Shaul, P. W., Yuhanna, I. S., Conrad, P. A. and Smart, E. J. (1999). Oxidized low density lipoprotein displaces endothelial nitric-oxide synthase (eNOS) from plasmalemmal caveolae and impairs eNOS activation. *J. Biol. Chem.* **274**, 32512-32519.
- Brochard-Wyart, F., Borghi, N., Cuvelier, D. and Nасsoy, P. (2006). Hydrodynamic narrowing of tubes extruded from cells. *Proc. Natl. Acad. Sci. USA* **103**, 7660-7663.
- Bruet, P. and McConnell, H. M. (1976). Lateral hapten mobility and immunochemistry of model membranes. *Proc. Natl. Acad. Sci. USA* **73**, 2977-2981.
- Butt, H. J. and Jaschke, M. (1995). Calculation of thermal noise in atomic-force microscopy. *Nanotechnology* **6**, 1-7.
- Byfield, F. J., Espinoza, H. A., Romanenko, V. G., Rothblat, G. H. and Levitan, I. (2004). Cholesterol depletion increases membrane stiffness of aortic endothelial cells. *Biophys. J.* **87**, 3336-3343.
- Byfield, F. J., Tikku, S., Rothblat, G. H., Gooch, K. J. and Levitan, I. (2006). OxLDL increases endothelial stiffness, force generation, and network formation. *J. Lipid Res.* **47**, 715-723.
- Chien, S. and Shyy, J. Y. (1998). Effects of hemodynamic forces on gene expression and signal transduction in endothelial cells. *Biol. Bull.* **194**, 390-391; discussion 392-393.
- Cooper, R. A. (1978). Influence of increased membrane cholesterol on membrane fluidity and cell function in human red blood cells. *J. Supramol. Struct.* **8**, 413-430.
- Cybulsky, M. I. and Gimbrone, M. A., Jr (1991). Endothelial expression of a mononuclear leukocyte adhesion molecule during atherogenesis. *Science* **251**, 788-791.
- Dai, J. and Sheetz, M. P. (1995). Mechanical properties of neuronal growth cone membranes studied by tether formation with laser optical tweezers. *Biophys. J.* **68**, 988-996.
- Dai, J., Sheetz, M. P., Wan, X. and Morris, C. E. (1998). Membrane tension in swelling and shrinking molluscan neurons. *J. Neurosci.* **18**, 6681-6692.
- Dai, J., Beall, H. P. T., Hochmuth, R. M., Sheetz, M. P. and Titus, M. A. (1999). Myosin I contributes to the generation of resting cortical tension. *Biophys. J.* **77**, 1168-1176.
- Davies, M. G., Berkowitz, D. E. and Hagen, P. O. (1995). Constitutive nitric oxide synthase is expressed and nitric oxide-mediated relaxation is preserved in retrieved human aortocoronary vein grafts. *J. Surg. Res.* **58**, 732-738.
- Edidin, M., Zagysky, Y. and Lardner, T. J. (1976). Measurement of membrane protein lateral diffusion in single cells. *Science* **191**, 466-468.
- Edmondson, K. E., Denney, W. S. and Diamond, S. L. (2005). Neutrophil-bead collision assay: pharmacologically induced changes in membrane mechanics regulate the PSGL-1/P-selectin adhesion lifetime. *Biophys. J.* **89**, 3603-3614.
- Evans, E. and Needham, D. (1987). Physical properties of surfactant bilayer membranes: thermal transition, elasticity, rigidity, cohesion and colloidal interactions. *J. Phys. Chem. 91*, 4219-4228.
- Evans, E., Heinrich, V., Leung, A. and Kinoshita, K. (2005). Nano- to microscale dynamics of P-selectin detachment from leukocyte interfaces. I. Membrane separation from the cytoskeleton. *Biophys. J.* **88**, 2288-2298.
- Gimbrone, M. A., Jr, Cybulsky, M. I., Kume, N., Collins, T. and Resnick, N. (1995). Vascular endothelium. An integrator of pathophysiological stimuli in atherogenesis. *Ann. N. Y. Acad. Sci.* **748**, 122-131; discussion 131-132.
- Girdhar, G. and Shao, J. Y. (2004). Membrane tether extraction from human umbilical vein endothelial cells and its implication in leukocyte rolling. *Biophys. J.* **87**, 3561-3568.
- Girdhar, G., Chen, Y. and Shao, J. Y. (2007). Double-tether extraction from human umbilical vein and dermal microvascular endothelial cells. *Biophys. J.* **92**, 1035-1045.

- Goodwin, J. S., Drake, K. R., Rimmert, C. L. and Kenworthy, A. K. (2005). Ras diffusion is sensitive to plasma membrane viscosity. *Biophys. J.* **89**, 1398-1410.
- Heinrich, V. and Waugh, R. E. (1996). A piconewton force transducer and its application to measurement of the bending stiffness of phospholipid membranes. *Ann. Biomed. Eng.* **24**, 595-605.
- Heinrich, V., Leung, A. and Evans, E. (2005). Nano- to microscale dynamics of P-selectin detachment from leukocyte interfaces. II. Tether flow terminated by P-selectin dissociation from PSGL-1. *Biophys. J.* **88**, 2299-2308.
- Hochmuth, F. M., Shao, J. Y., Dai, J. and Sheetz, M. P. (1996). Deformation and flow of membrane into tethers extracted from neuronal growth cones. *Biophys. J.* **70**, 358-369.
- Hochmuth, R. M., Wiles, H. C., Evans, E. and McCown, J. T. (1982). Extensional flow of erythrocyte membrane from cell body to elastic tether. *Biophys. J.* **39**, 83-89.
- Hosu, B. G., Sun, M., Marga, F., Grandbois, M. and Forgacs, G. (2007). Eukaryotic membrane tethers revisited using magnetic tweezers. *Phys. Biol.* **4**, 67-78.
- Hutter, J. L. and Bechhoefer, J. (1993). Calibration of atomic-force microscope tips. *Rev. Sci. Instrum.* **64**, 1868-1873.
- Inaba, T., Ishijima, A., Honda, M., Nomura, F., Takiguchi, K. and Hotani, H. (2005). Formation and maintenance of tubular membrane projections require mechanical force, but their elongation and shortening do not require additional force. *J. Mol. Biol.* **348**, 325-333.
- Kenworthy, A. K., Nichols, B. J., Rimmert, C. L., Hendrix, G. M., Kumar, M., Zimmerberg, J. and Schwartz, J. L. (2004). Dynamics of putative raft-associated proteins at the cell surface. *J. Cell Biol.* **165**, 735-746.
- Kwik, J., Boyle, S., Fooksman, D., Margolis, L., Sheetz, M. P. and Edidin, M. (2003). Membrane cholesterol, lateral mobility, and the phosphatidylinositol 4,5-bisphosphate-dependent organization of cell actin. *Proc. Natl. Acad. Sci. USA* **100**, 13964-13969.
- Levitan, I., Christian, A. E., Tulenko, T. N. and Rothblat, G. H. (2000). Membrane cholesterol content modulates activation of volume-regulated anion current in bovine endothelial cells. *J. Gen. Physiol.* **115**, 405-416.
- Li, Z., Anvari, B., Takashima, M., Brecht, P., Torres, J. H. and Brownell, W. E. (2002). Membrane tether formation from outer hair cells with optical tweezers. *Biophys. J.* **82**, 1386-1395.
- Lowry, O. H., Rosebrough, N. J., Farr, A. L. and Randall, R. J. (1951). Protein measurement with the Folin phenol reagent. *J. Biol. Chem.* **193**, 265-275.
- Marcus, W. D. and Hochmuth, R. M. (2002). Experimental studies of membrane tethers formed from human neutrophils. *Ann. Biomed. Eng.* **30**, 1273-1280.
- Needham, D. and Nunn, R. S. (1990). Elastic deformation and failure of lipid bilayer membranes containing cholesterol. *Biophys. J.* **58**, 997-1009.
- Neter, J., Michael, H. K., William, W. and Christopher, J. N. (1996). *Applied Linear Statistical Models*. Burr Ridge, IL: McGraw-Hill/Irwin.
- Polishchuk, E. V., Di Pentima, A., Luini, A. and Polishchuk, R. S. (2003). Mechanism of constitutive export from the golgi: bulk flow via the formation, protrusion, and en bloc cleavage of large trans-golgi network tubular domains. *Mol. Biol. Cell* **14**, 4470-4485.
- Pritchard, K. A., Jr, Schwarz, S. M., Medow, M. S. and Stemberman, M. B. (1991a). Effect of low-density lipoprotein on endothelial cell membrane fluidity and mononuclear cell attachment. *Am. J. Physiol. Cell Physiol.* **260**, C43-C49.
- Pritchard, K. A., Jr, Tota, R. R., Lin, J. H., Danishefsky, K. J., Kurilla, B. A., Holland, J. A. and Stemberman, M. B. (1991b). Native low density lipoprotein. Endothelial cell recruitment of mononuclear cells. *Arterioscler. Thromb.* **11**, 1175-1181.
- Puech, P.-H., Taubenberger, A., Ulrich, F., Krieg, M., Muller, D. J. and Heisenberg, C.-P. (2005). Measuring cell adhesion forces of primary gastrulating cells from zebrafish using atomic force microscopy. *J. Cell Sci.* **118**, 4199-4206.
- Ramachandran, V., Williams, M., Yago, T., Schmidtke, D. W. and McEver, R. P. (2004). Dynamic alterations of membrane tethers stabilize leukocyte rolling on P-selectin. *Proc. Natl. Acad. Sci. USA* **101**, 13519-13524.
- Raucher, D. and Sheetz, M. P. (1999). Characteristics of a membrane reservoir buffering membrane tension. *Biophys. J.* **77**, 1992-2002.
- Raucher, D. and Sheetz, M. P. (2000). Cell spreading and lamellipodial extension rate is regulated by membrane tension. *J. Cell Biol.* **148**, 127-136.
- Raucher, D. and Sheetz, M. P. (2001). Phospholipase C activation by anesthetics decreases membrane-cytoskeleton adhesion. *J. Cell Sci.* **114**, 3759-3766.
- Raucher, D., Stauffer, T., Chen, W., Shen, K., Guo, S., York, J. D., Sheetz, M. P. and Meyer, T. (2000). Phosphatidylinositol 4,5-bisphosphate functions as a second messenger that regulates cytoskeleton-plasma membrane adhesion. *Cell* **100**, 221-228.
- Reits, E. A. and Neeffjes, J. J. (2001). From fixed to FRAP: measuring protein mobility and activity in living cells. *Nat. Cell Biol.* **3**, E145-E147.
- Rosenfeld, M. E., Tsukada, T., Gown, A. M. and Ross, R. (1987). Fatty streak initiation in Watanabe Heritable Hyperlipemic and comparably hypercholesterolemic fat-fed rabbits. *Arteriosclerosis* **7**, 9-23.
- Rustom, A., Saffrich, R., Markovic, I., Walther, P. and Gerdes, H. H. (2004). Nanotubular highways for intercellular organelle transport. *Science* **303**, 1007-1010.
- Saffman, P. G. and Delbruck, M. (1975). Brownian motion in biological membranes. *Proc. Natl. Acad. Sci. USA* **72**, 3111-3113.
- Schmidtke, D. W. and Diamond, S. L. (2000). Direct observation of membrane tethers formed during neutrophil attachment to platelets or P-selectin under physiological flow. *J. Cell Biol.* **149**, 719-730.
- Shao, J. Y. and Hochmuth, R. M. (1996). Micropipette suction for measuring piconewton forces of adhesion and tether formation from neutrophil membranes. *Biophys. J.* **71**, 2892-2901.
- Shao, J. Y. and Xu, J. (2002). A modified micropipette aspiration technique and its application to tether formation from human neutrophils. *J. Biomech. Eng.* **124**, 388-396.
- Shao, J.-Y., Ting-Beall, H. P. and Hochmuth, R. M. (1998). Static and dynamic lengths of neutrophil microvilli. *Proc. Natl. Acad. Sci. USA* **95**, 6797-6802.
- Sharma, D. K., Brown, J. C., Choudhury, A., Peterson, T. E., Holicky, E., Marks, D. L., Simari, R., Parton, R. G. and Pagano, R. E. (2004). Selective stimulation of caveolar endocytosis by glycosphingolipids and cholesterol. *Mol. Biol. Cell* **15**, 3114-3122.
- Sheetz, M. P. (2001). Cell control by membrane-cytoskeleton adhesion. *Nat. Rev. Mol. Cell Biol.* **2**, 392-396.
- Sheetz, M. P., Sable, J. E. and Dobreiner, H. G. (2006). Continuous membrane-cytoskeleton adhesion requires continuous accommodation to lipid and cytoskeleton dynamics. *Annu. Rev. Biophys. Biomol. Struct.* **35**, 417-434.
- Shvartsman, D. E., Gutman, O., Tietz, A. and Hennis, Y. I. (2006). Cyclodextrins but not compactin inhibit the lateral diffusion of membrane proteins independent of cholesterol. *Traffic* **7**, 917-926.
- Sieminski, A. L., Hebbel, R. P. and Gooch, K. J. (2004). The relative magnitudes of endothelial force generation and matrix stiffness modulate capillary morphogenesis in vitro. *Exp. Cell Res.* **297**, 574-584.
- Siggia, E. D., Schwartz, J. L. and Bekiranov, S. (2000). Diffusion in inhomogeneous media: theory and simulations applied to whole cell photobleach recovery. *Biophys. J.* **79**, 1761-1770.
- Spector, L., Shochet, N. R., Blasberger, D. and Kashman, Y. (1989). Latrunculin—novel marine macrolides that disrupt microfilament organization and affect cell growth: I. Comparison with cytochalasin D. *Cell Motil. Cytoskeleton* **13**, 127-144.
- Subtil, A., Gaidarov, I., Kobylarz, K., Lampson, M. A., Keen, J. H. and McGraw, T. E. (1999). Acute cholesterol depletion inhibits clathrin-coated pit budding. *Proc. Natl. Acad. Sci. USA* **96**, 6775-6780.
- Sun, M., Graham, J. S., Hegedus, B., Marga, F., Zhang, Y., Forgacs, G. and Grandbois, M. (2005). Multiple membrane tethers probed by atomic force microscopy. *Biophys. J.* **89**, 4320-4329.
- Titushkin, I. and Cho, M. (2006). Distinct membrane mechanical properties of human mesenchymal stem cells determined using laser optical tweezers. *Biophys. J.* **90**, 25282-2591.
- Upadhyaya, A. and Sheetz, M. P. (2004). Tension in tubulovesicular networks of Golgi and endoplasmic reticulum membranes. *Biophys. J.* **86**, 2923-2928.
- Vidulescu, C., Clejan, S. and O'Connor, K. C. (2004). Vesicle traffic through intercellular bridges in DU 145 human prostate cancer cells. *J. Cell. Mol. Med.* **8**, 388-396.
- Vrljic, M., Nishimura, S. Y., Moerner, W. E. and McConnell, H. M. (2005). Cholesterol depletion suppresses the translational diffusion of class II major histocompatibility complex proteins in the plasma membrane. *Biophys. J.* **88**, 334-347.
- White, J., Johannes, L., Mallard, F., Girod, A., Grill, S., Reinsch, S., Keller, P., Tzschaschel, B., Echard, A., Goud, B. et al. (1999). Rab6 coordinates a novel Golgi to ER retrograde transport pathway in live cells. *J. Cell Biol.* **147**, 743-760.
- Xu, G. and Shao, J. Y. (2005). Double tether extraction from human neutrophils and its comparison with CD4+ T-lymphocytes. *Biophys. J.* **88**, 661-669.
- Xu, X. and London, E. (2000). The effect of sterol structure on membrane lipid domains reveals how cholesterol can induce lipid domain formation. *Biochemistry* **39**, 843-849.
- Zar, J. H. (1999). *Biostatistical Analysis*. Upper Saddle River, NJ: Prentice Hall.
- Zhelev, D. V. and Hochmuth, R. M. (1995). Mechanically stimulated cytoskeleton rearrangement and cortical contraction in human neutrophils. *Biophys. J.* **68**, 2004-2014.